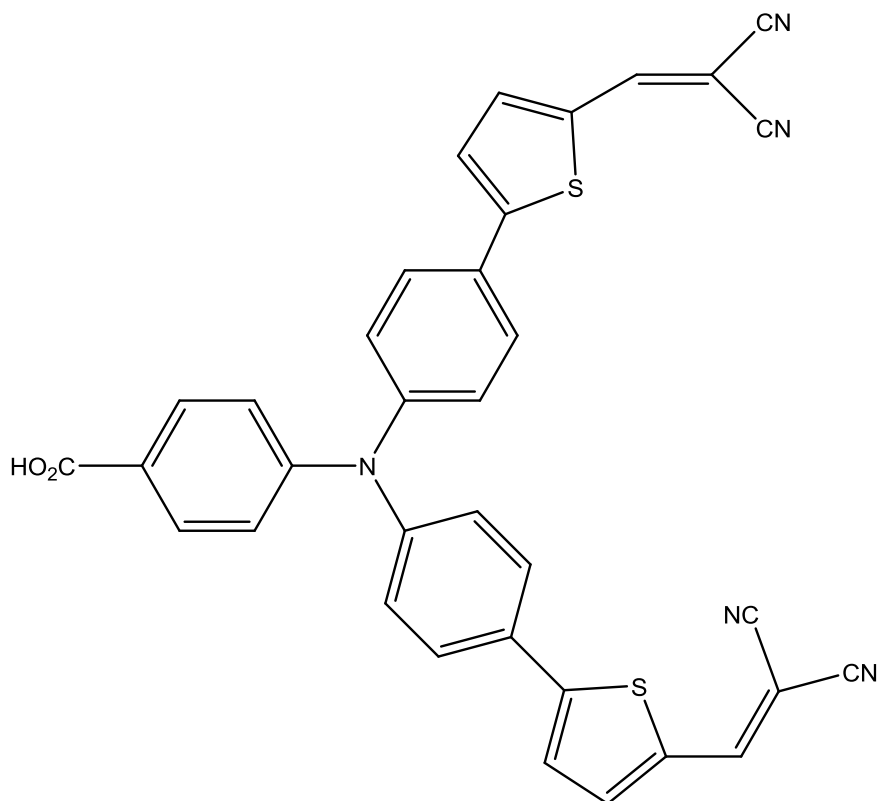


## Supplementary Information

### Dye sensitised solar cells with nickel oxide photocathodes prepared via scalable microwave sintering

Elizabeth A. Gibson, Muhammad Awais, Danilo Dini, Denis P. Dowling, Mary T. Pryce, Johannes G. Vos, Gerrit Boschloo, Anders Hagfeldt



**Figure S10.** Structure of the dye-sensitizer **P1**.

The redox properties of **P1** (Figure S10) have been evaluated and the electrochemical data reproduce those reported in ref. 4b. The oxidation peaks of **P1** in solution at 0.7 and 1.3 V vs Fc<sup>+</sup>/Fc do not overlap with those of NiOx (range of electroactivity: 0-0.8 V vs Fc<sup>+</sup>/Fc). The details of the synthesis of **P1** have been reported in ref. 4c. **P1** in acetonitrile presents two main absorption peaks at 340 and 475 nm.

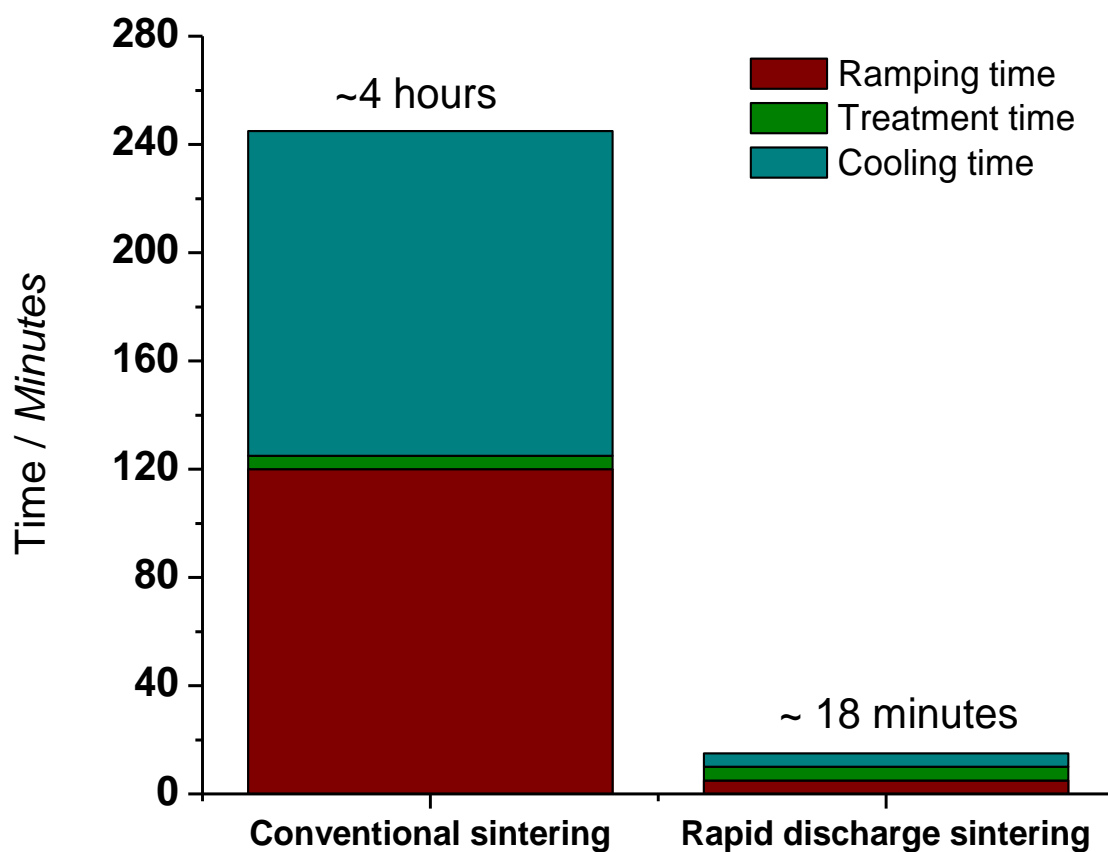


**Figure S11.** Comparison of the processing times for CS and RDS sintering procedures when the deposition of  $\text{NiO}_x$  thin films for DSCs is considered.

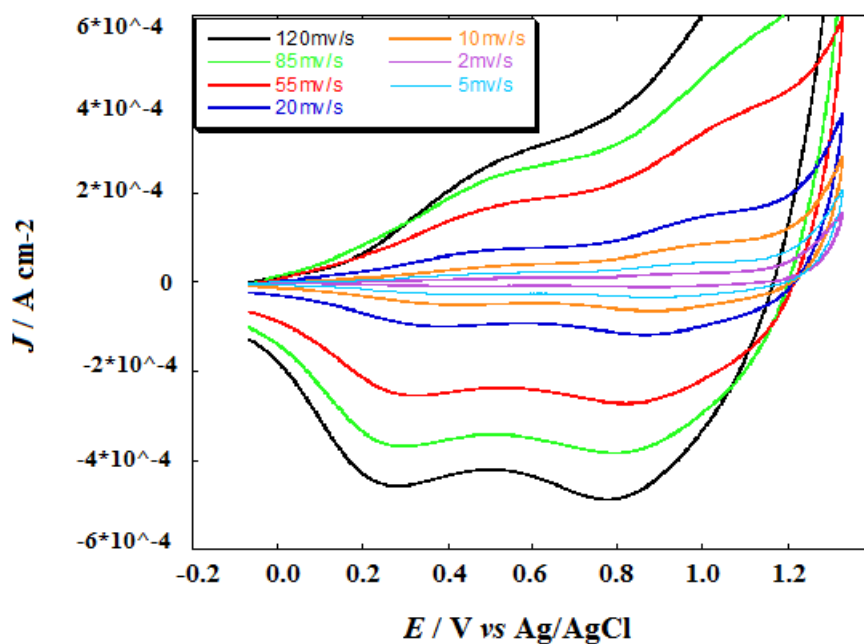


**Figure SI2a.** Voltammetric profiles of NiO sample **1** with thickness  $a$  ( $l$ :  $0.4 \mu\text{m}$ ) at different scan rates. Counter electrode: Pt; electrolyte composition:  $0.2 \text{ M KCl}$ ,  $0.01 \text{ M KH}_2\text{PO}_4$  and  $0.01 \text{ M K}_2\text{HPO}_4$  in water.

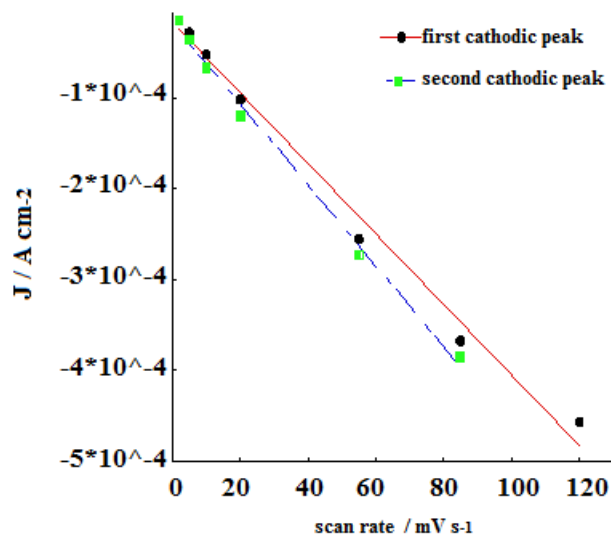


**Figure SI2b.** Linear scan rate dependence of the two cathodic peaks of NiO sample **1** with  $l$ :  $0.4 \mu\text{m}$  from data of Figure SI2a. First and second cathodic peaks are centered at *ca.*  $0.25$  and  $0.82 \text{ V vs Ag/AgCl}$ , respectively.

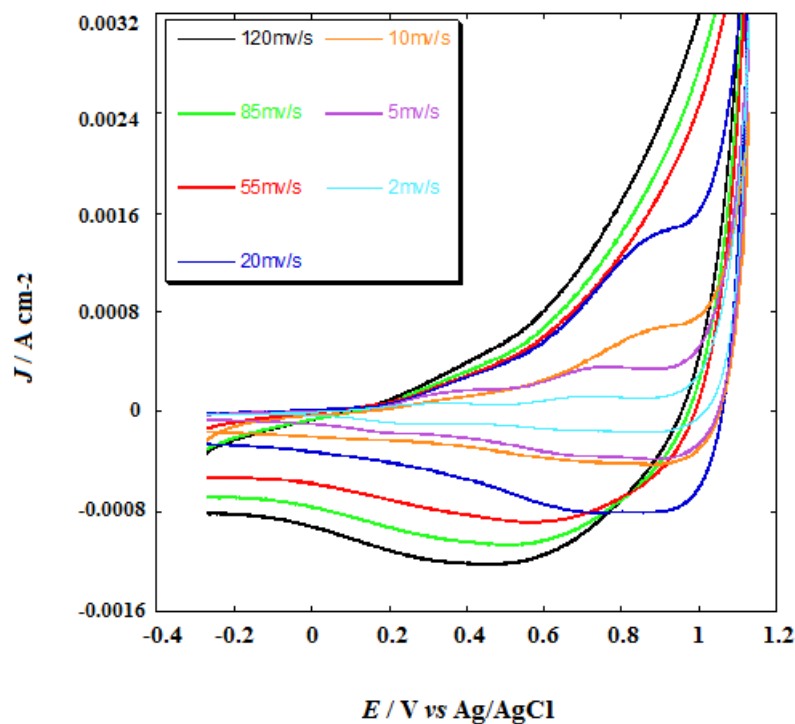


**Figure SI3a.** Voltammetric profiles of NiO sample 2 with thickness  $a$  ( $l$ : 0.4  $\mu\text{m}$ ) at different scan rates. Counter electrode: Pt; electrolyte composition: 0.2 M KCl, 0.01 M KH<sub>2</sub>PO<sub>4</sub> and 0.01 M K<sub>2</sub>HPO<sub>4</sub> in water.

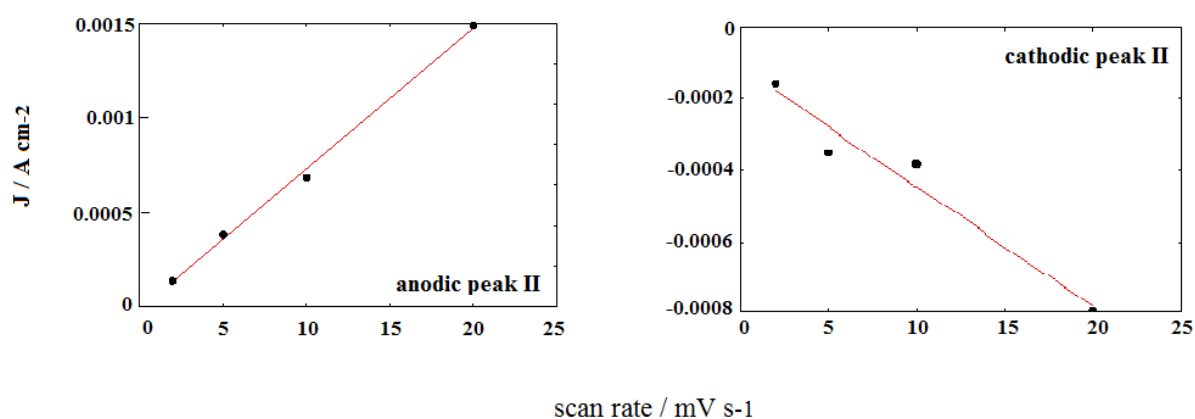
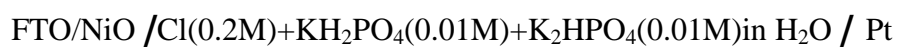


**Figure SI3b.** Linear scan rate dependence of (left) anodic and (right) cathodic peak II of NiO sample 2 with  $l$ : 0.4  $\mu\text{m}$  (data from Figure SI3a). Peak II is centred at approximately 0.74 V vs Ag/AgCl.

The open circuit potential,  $V_{OC}$ , of the cell



is reported in Table S11. The striking difference between the  $V_{OC}$  value of the thinner films **a** and films **b** and **c** reflects the influence of the underlying FTO substrate in the determination of  $V_{OC}$  for samples **a**. These findings are coherent with the fact that FTO is not uniformly covered by the thinnest NiO film **a** when  $l : 0.4 \mu\text{m}$ , and the substrate gets in direct contact with the electrolyte.

When the ratio ( $\gamma$ ) of oxidation peak I to oxidation peak II (Table S11, data from Figure 4) is considered an empirical parameter indicative of the degree of crystallinity present in nanostructured NiO films [5] being  $\gamma \geq 1$  in single crystals [22b], we find that the NiO films sintered with CS and RDS methods possess generally low crystallinity with  $\gamma$  ranging in the interval  $0.6 < \gamma < 0.8$  for NiO samples **1** and **2**.

Sample	$V_{OC} / \text{V}$	$\gamma = J_p(\text{I}) / J_p(\text{II})$
<b>1a</b>	-0.47	0.71
<b>1b</b>	0.33	0.67
<b>1c</b>	0.28	0.72
<b>2a</b>	-0.51	0.71
<b>2b</b>	0.29	0.63
<b>2c</b>	0.28	0.78

**Table S11.** Open circuit voltage,  $V_{OC}$ , and ratio  $J_p(\text{I})$  to  $J_p(\text{II})$  (Table 2),  $\gamma$ , for bare NiO samples **1** and **2** with different thicknesses **a-c**.  $V_{OC}$  values are referred to the redox couple Ag/AgCl.

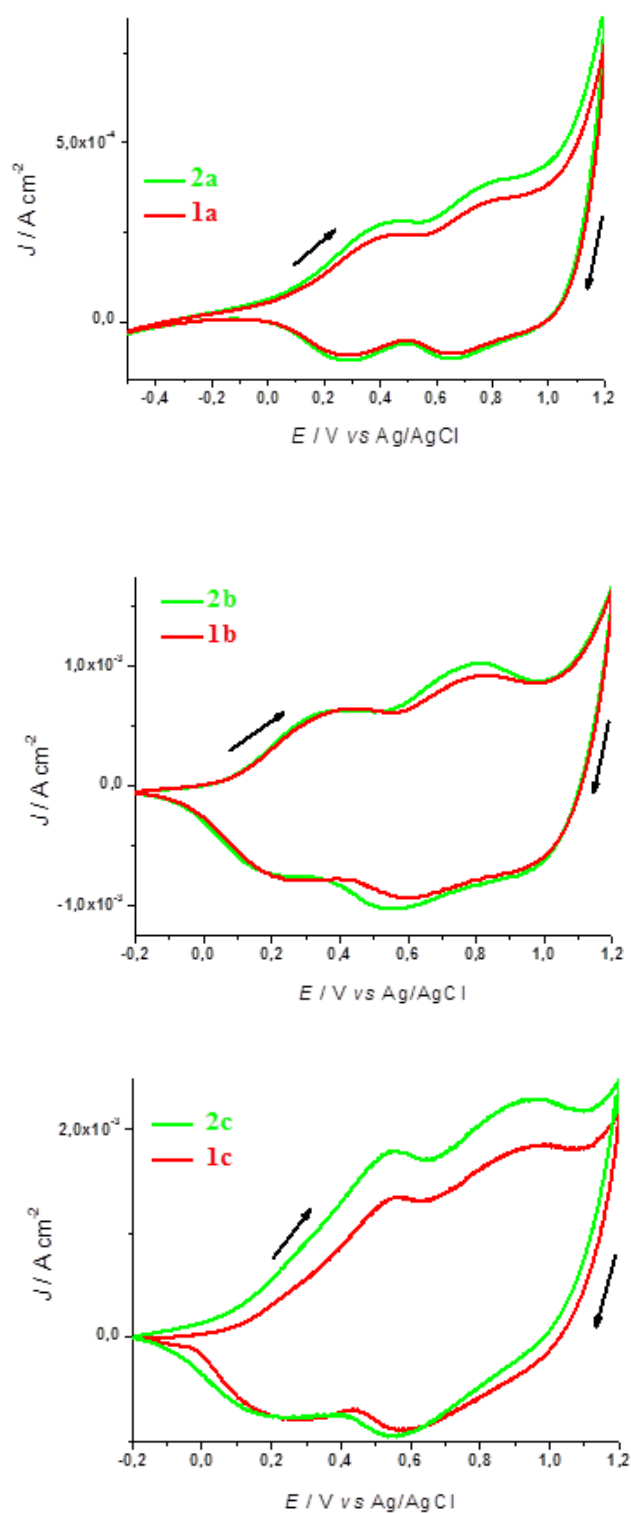


**Figure SI4.** Comparison of the cyclic voltammograms of NiO samples **1** and **2** having the same thickness. Data taken from Figure 4. Arrows indicate the direction of potential scan.

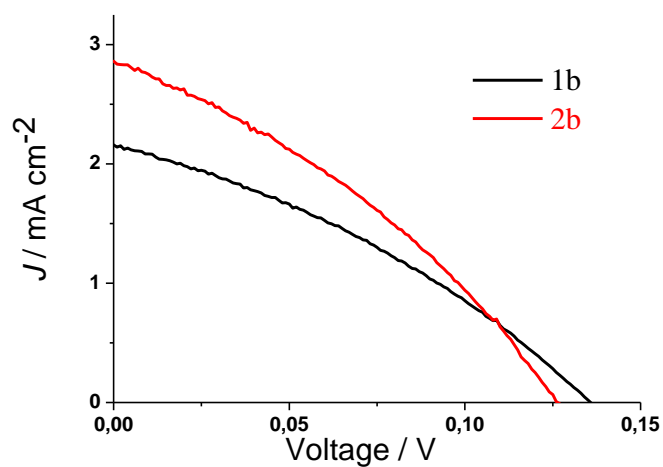


**Figure SI5.**  $J$ - $V$  curves under illumination for  $p$ -DSCs assembled with NiO samples **1** and **2** having the same thickness **b**.

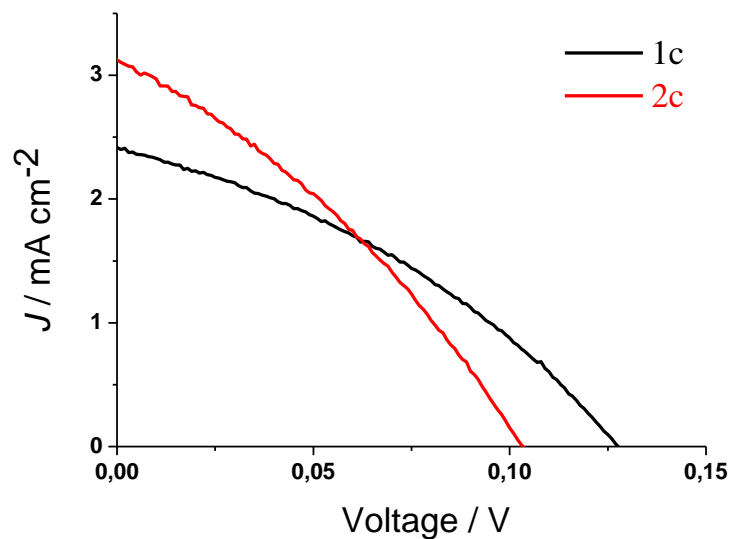


**Figure SI6.**  $J$ - $V$  curves under illumination for  $p$ -DSCs assembled with NiO samples **1** and **2** having the same thickness **c**.

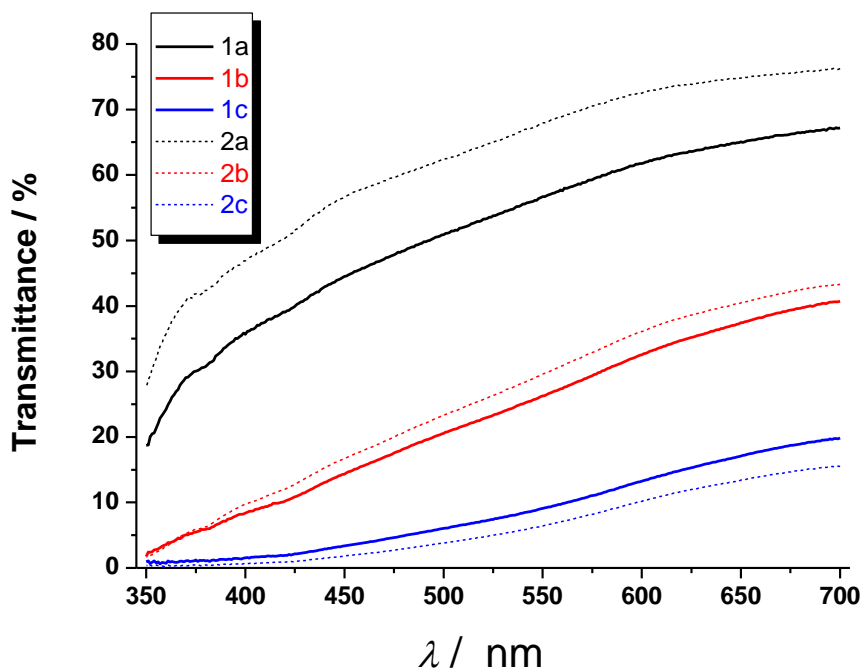


**Figure SI7.** Transmission spectra of bare NiO samples **1** and **2** at the three different thicknesses **a-c**. The generally higher transmittance of samples **2** in the thickness range  $0.4 \leq l \leq 2.0 \mu\text{m}$  is indicative of the lower density and reduced scattering phenomena in RDS samples **2** vs CS samples **1** as expected from the analysis of the morphological features (Figures 1 and 2).



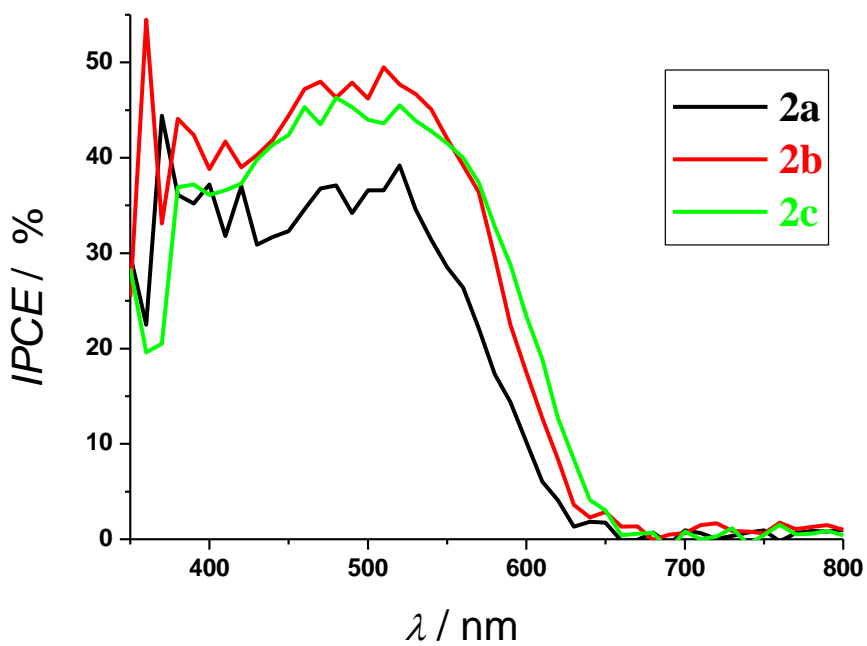
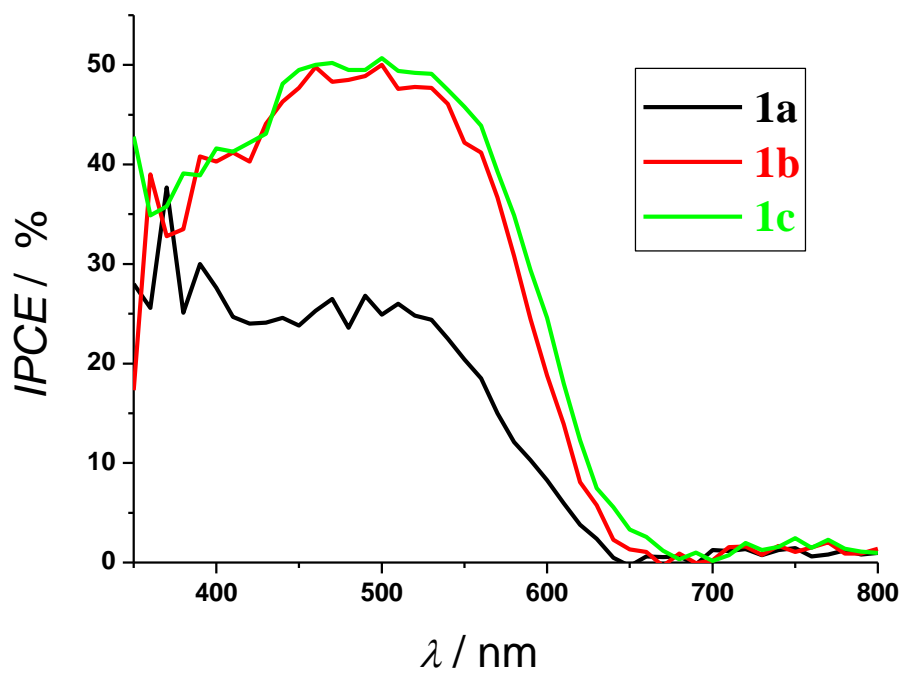


**Figure S18.** IPCE spectra of P1-sensitized NiO samples **1** (upper graph) and **2** (lower graph) at the three different thicknesses **a-c**.

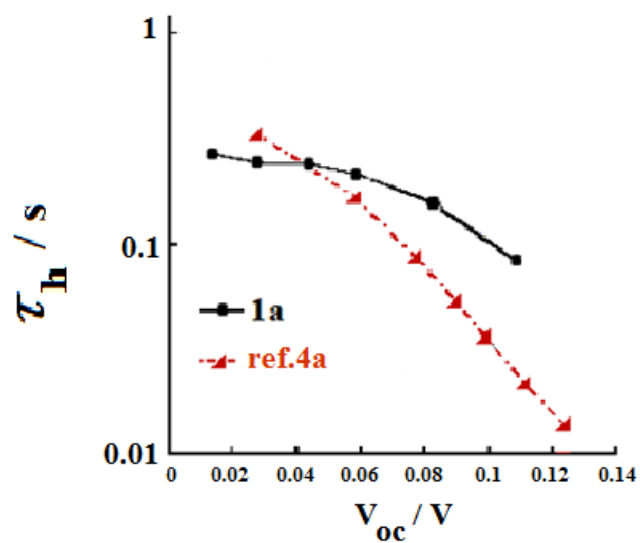


**Figure SI9.** Hole lifetime ( $\tau_h$ ) vs open circuit photovoltage  $V_{oc}$  plot for a *p*-DSC assembled with NiO sample **1a** sensitized with P1, and data from ref.4a referring to a sample with comparable thickness.